ORIGINAL PAPER

Sedimentological and sequence-stratigraphic analyses of the Tithonian Hith Anhydrite Formation in the Dahal Hit outcrop, Saudi Arabia

Philipp J. Wolpert[1] · Martin Bartenbach[2] · Thomas Aigner[3] · Augustus O. Wilson[4] · Moujahed I. Al-Husseini[5,6] · Alexander Petrovic[7] · Heiko Dirks[8] · Randolf Rausch[9]

Abstract

The Dahal Hit cavern in Central Saudi Arabia is the only locality where the Tithonian Hith Anhydrite Formation is exposed in the Middle East. In 2010, a 28.5-m interval in the 90-m-thick Hith Formation was logged and described in the cavern as part of a study to evaluate its sedimentological and sequence-stratigraphic architecture and to identify potential high-permeability layers within the seal of the world's most prolific petroleum system. Seven facies types were interpreted as reflecting sabkha (subaerial) or salina (subaqueous) settings, and their vertical stacking patterns revealed that the logged interval consists of three transgressive–regressive cycles and part of a fourth cycle. The cavern was revisited in 2016 but only to find that the water level had risen by about 50 m rendering further geological studies impossible. The higher level of the water suggests that the cavern was flooded by the flow in the subsurface of treated sewage water released into a former quarry. The quarry is situated about 10 km southeast of the cavern, and the storage of water in it started in 2008. The flow pathways to the Dahal Hit cavern are apparently well-connected karsts, caverns, and high-permeability flow zones present in dolomite layers.

1   Vulcan Energy Subsurface Solutions, Karlsruhe, Germany

2   Equinor ASA, Trondheim, Norway

3   Eberhard Karls University, Tübingen, Germany

4   Consulting Geologist, London, UK

5   GeoArabia, Manama, Bahrain

6   Aramco, Dhahran, Saudi Arabia

7   Carmeuse, Louvain-La-Neuve, Belgium

8   Ingenieurgesellschaft Prof. Kobus Und Partner GmbH, Stuttgart, Germany

9   Institute of Applied Geosciences, Technische Universität Darmstadt, Darmstadt, Germany

Introduction

Several countries on the Arabian Peninsula, such as Saudi Arabia, are developing and deploying technologies aimed at CO_2 capture, utilization, and storage (CCUS) in candidate formations (Fedorik et al. 2023; Vahrenkamp et al. 2021; Oelkers et al. 2022). The Upper Jurassic Hith Anhydrite Formation in Saudi Arabia has been considered a potential candidate for a CCUS project because storing CO_2 in it would also maintain pressure in its intra-formation reservoirs and those in the underlying Upper Jurassic Arab Formation. Furthermore, the Hith Anhydrite Formation is considered a regional aquitard, which separates two mega-aquifer systems (Rausch et al 2013; Rausch and Dirks 2024); however, the continuity and homogeneity of the aquitard properties across some regions in the Arabian Platform have not been quantitatively established.

This study is aimed at characterizing the formation's stratigraphy in the subsurface and in its type locality in the Dahal Hit dissolution cavern. The cavern is located approximately 30 km south of Ar Riyadh at the foot of Jabal Hit escarpment (Fig. 1). The cavern and escarpment are the only

Fig. 1 Satellite image showing the location of the Dahal Hit cavern and the Hith-Sulaiy type locality Dahal Hit

locality where the Tithonian Hith Formation of the Shaqra Group and the overlying Tithonian-Berriasian Sulaiy Formation of the Thamama Group are exposed in Saudi Arabia (Powers et al. 1966; Powers 1968; Wolpert et al. 2015).

As part of our study, some of the authors descended into the Dahal Hit cavern and recorded the groundwater level in 2010 and again in 2016 (Fig. 2) and noticed that it had risen by c. 50 m implying an average rise of about 8 m per year. This increase constitutes a significant change in our understanding of the Upper Jurassic hydrogeological system; it suggests that the cavern was flooded by treated sewage water released into a former quarry situated about

Fig. 2 Stratigraphic column showing the age of the Hith Anhydrite Formation based on the International Chronostratigraphic Chart 2023/04 of the International Commission on Stratigraphy (www.stratigraphy.org). The schematic sketch of the Dahal Hit dissolution cavern in the study area is modified from Wilson (2020). Positions of Jurassic maximum flooding surfaces MFS J10 and MFS J11 and Cretaceous MFS K10 after Wolpert et al. (2015)
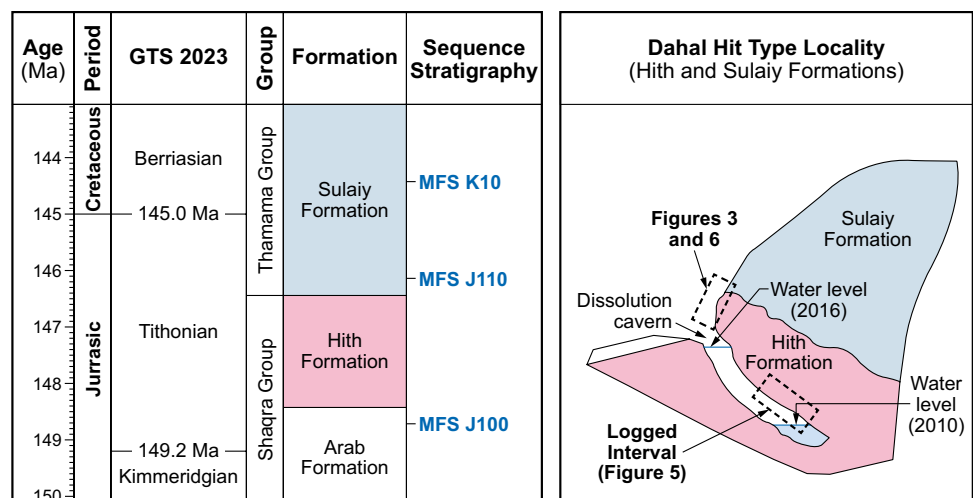
10 km southeast of the cavern starting in 2008 (Michelsen et al. 2016).

In this likely scenario, the rapid rise in water level implies that a well-developed and well-connected flow-zone network is present in the Hith Anhydrite Formation, and probably in the carbonates of the underlying Arab and overlying Sulaiy Formations. To better understand the stratigraphy of the Hith Formation, this study characterizes its facies types, interprets its sedimentological and sequence-stratigraphic architecture, and investigates the potential structural and stratigraphic intra-Hith flow zones as well as the lateral continuity of geobodies. Such information can only be partly derived from cores, and hence, the outcrop at Dahal Hith provides a unique opportunity to investigate these features.

Data and methods

The entrance to the Dahl Hit cavern is a gap between large boulders (Fig. 3). Once inside, the cavern becomes much wider, and lateral and vertical facies trends are evident over several 10 s of meters (Fig. 4). Despite the challenging and unstable conditions in the cavern, a vertical profile of 28.5 m was logged (approximately 1/3 of the total thickness of the Hith Formation) and described at a 1:20 scale in 2010. The natural gamma radiation along the logged profile was measured at 20 cm sample spacing and a period of 20 s by a portable gamma ray device (model GS-256) (Fig. 5).

Sedimentary structures and textures are well pronounced and are used for facies interpretation in this study. An

Fig. 3 Entrance of the Dahal Hit cavern and the transition from the Hith to Sulaiy Formation

Fig. 4 View of the outcrop inside the Dahal Hit cavern
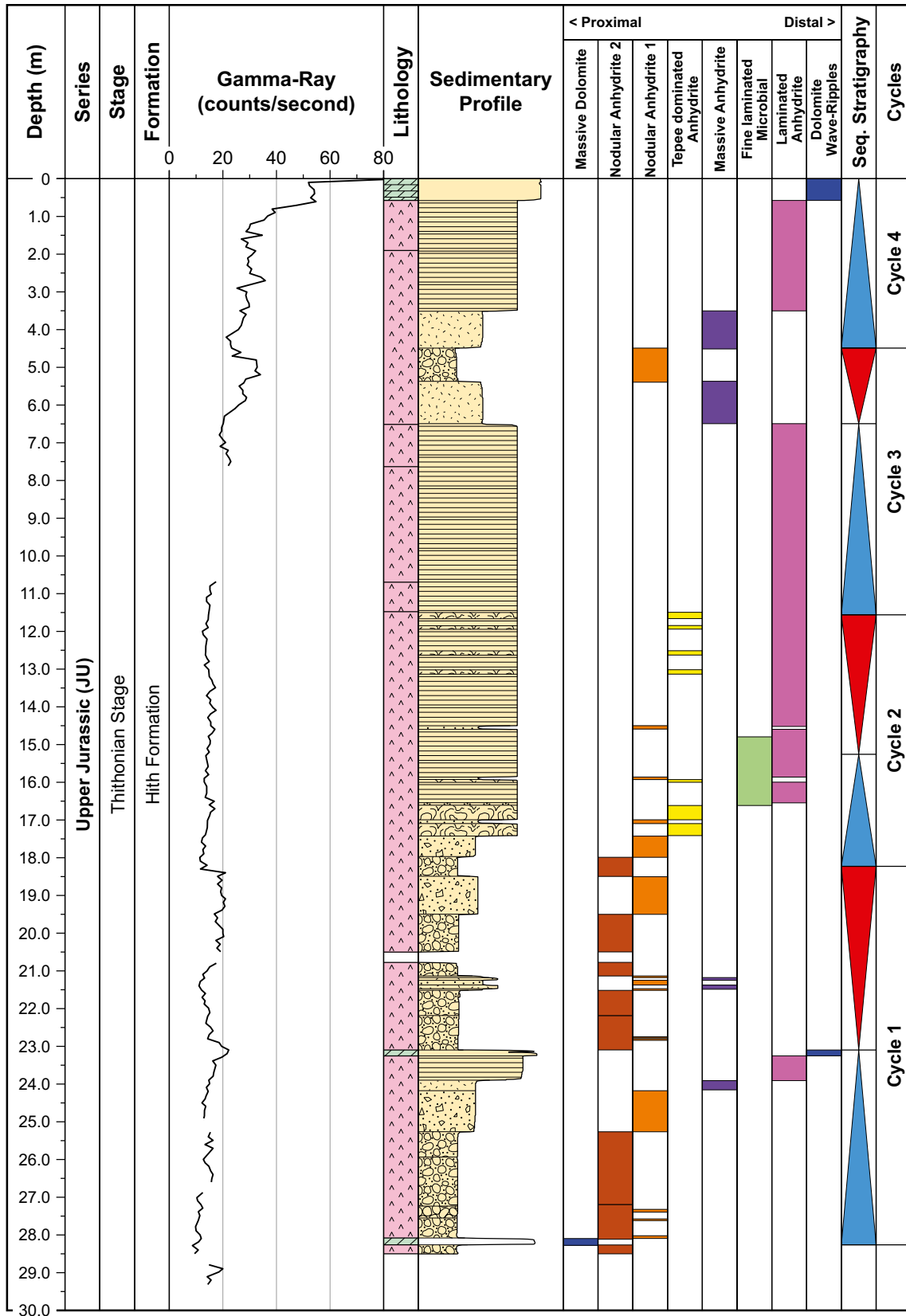
Fig. 5 Sedimentological profile, gamma ray log, and sequence-stratigraphic interpretation based on facies stacking pattern analyses. See "Cycles in Dahl Hit cavern" for discussion of cycles 1 to 4

interpreted vertical chart is shown in Fig. 5, which represents the proximal–distal arrangements of the characterized lithofacies types. This chart provides a quick overview of stratigraphic trends and architecture in evaporites. Samples for thin section analysis could not be recovered from the outcrop conditions.

Hith Anhydrite Formation, Shaqra Group

According to Powers (1968), the Hith Formation was first recognized in an unpublished ARAMCO report by Bramkamp and Barger (1938, unpublished), amended by Powers et al. (1964, unpublished ARAMCO report), and formally defined in Powers et al. (1966) at Dahal Hit (Fig. 1).

Powers (1968) divided the formation into the informal "main Hith anhydrite" and overlying Manifa Reservoir, named after the discovery of oil at the Manifa field in 1957. The main Hith anhydrite is typically between 60 and 120 m thick and 90 m thick at the type section at Dahal Hit (Powers 1968). The main Hith anhydrite consists of massive, bedded anhydrite with minor intercalations of aphanitic limestone, dolomite, or calcarenite. The Manifa Reservoir occurs in northeastern Saudi Arabia, between the sharply defined top of the main Hith anhydrite and the base of the tight aphanitic limestone of the Sulaiy Formation (Powers 1968). The Manifa Reservoir, on average c. 18 m thick, is mainly oolitic calcarenite with variable amounts of nodular anhydrite, bedded anhydrite, and aphanitic carbonate.

Powers (1968) interpreted the contact between the Hith Formation and the underlying Arab Formation as conformable, and the contact with the overlying Sulaiy Formation as a possible disconformity (see the "Hith-Sulaiy transition and boundary" section). The Hith Anhydrite Formation is considered Tithonian based on stratigraphic position.

Hith-Sulaiy stratigraphy

Hith-Sulaiy transition and boundary

The transition between the Hith and Sulaiy formations is exposed at the entrance of the Dahal Hit cavern (Figs. 2, 3 and 6). The transition starts abruptly at the erosive "surface A" at the top of the Hith "laminated anhydrite" interval. Above surface A, "breccia 1" bed is about 1 m thick and consists predominantly of limestone clasts. The overlying section consists of a thin-bedded anhydrite bed bounded by "surfaces B and C" and "breccia 2" bed (2–3 m thick) consisting predominantly of limestone clasts. The upper "deformed anhydrite beds" start above "surface D" and represent the uppermost section of the transition. It is followed by the "evenly bedded limestone" beds of the Sulaiy Formation.

The stratigraphic position of the boundary between the Hith and Sulaiy at Dahal Hit is variously defined and interpreted. Steineke et al. (1958) placed it at surface A between the massive laminated anhydrite and the breccia 1 bed and interpreted the contact as an unconformity. Powers et al.

Fig. 6 The Hith-Sulaiy transition at the entrance of the Dahl Hit cavern (Figs. 2 and 3) is characterized by several lithological units bounded by surfaces A to D. Surface E represents the sequence boundary (SB) at base of the evenly bedded limestones of the Sulaiy Formation. See photos and captions in Figs. 7 and 8 for detailed description of the units
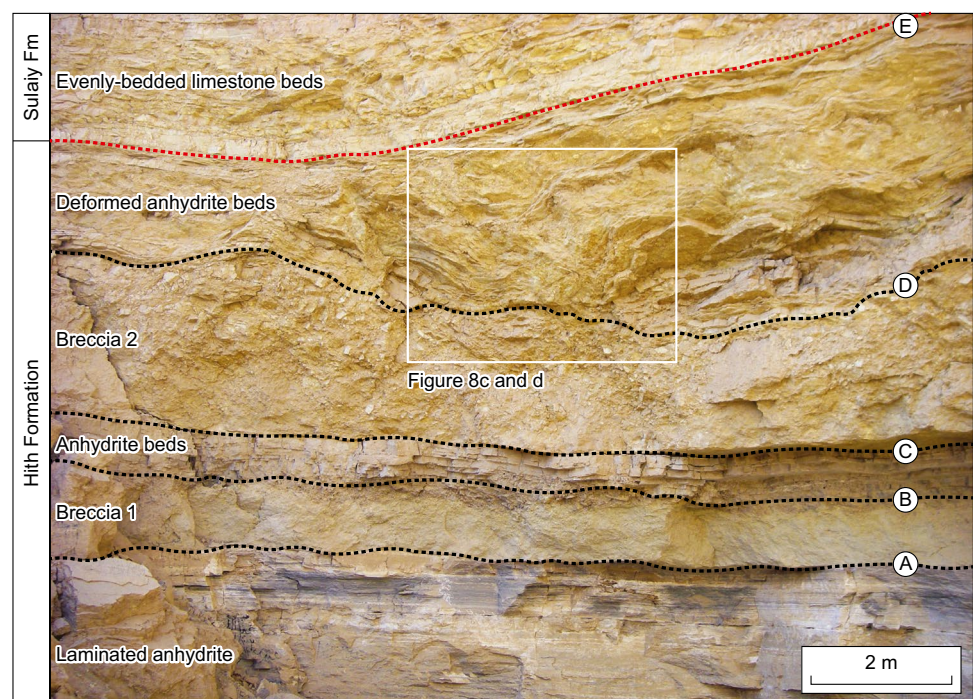
(1966) and Powers (1968), based on subsurface analyses, did not interpret the contact as a disconformity or unconformity. Instead, they interpreted the breccia intervals at Dahal Hit resulted from the dissolution of the intercalated anhydrite, which caused a solution collapse-type breccia. Vaslet et al. (1991, p. 15, caption in their fig. 8) interpreted the top of the Hith Anhydrite as a disconformity truncated by the basal beds of the Sulaiy Formation. Hughes and Naji (2008) described the Sulaiy-Hith transition in the offshore Manifa Field, located approximately 500 km northeast of Ar Riyadh in Saudi Arabia, and suggested that the boundary is a disconformity. Wolpert et al. (2015, this study) adopted a sequence-stratigraphic approach and placed the basal sequence boundary SB 1 of the Sulaiy transgression at surface E (Figs. 6, 7, and 8).

Results

Facies analyses

Alsharhan and Kendall (1994) discuss and compare the Upper Jurassic Hith facies with Holocene analogs. In this study, seven lithofacies types (LFT) have been identified within the investigated 28.5 m of the Hith Formation (Fig. 2). The main characteristics are summarized in Figs. 9 and 10 and discussed in detail in the following section.

LFT 1: nodular anhydrite (nodules touching)

Observation This facies type is characterized by the nodular texture of the anhydrite (Fig. 11). The texture is commonly referred to as "chicken-wire" (e.g., Alsharhan and Kendall 1994).

Fig. 7 Detailed photos and interpretations of the main sedimentological intervals in Fig. 6, starting from lowest unit in photos **a** and **b** and continuing in Fig. 8 upwards to the Sulaiy Formation. **a** Laminated anhydrite is largely composed of parallel-bedded centimeter to decimeter thick beds. **b** However, the blue dashed line in photo **b** indicates an individual layer, which is interpreted as enterolithic folds and/or tepee structures. **c** Breccia 1 erodes the laminated anhydrite as indicated by the lower red surface in photo **d**. Breccia 1 is composed of clasts typically 3 to 10 cm in size. **e** The anhydrite beds are parallel-bedded and several centimeters in thickness highlighted in photo **f**
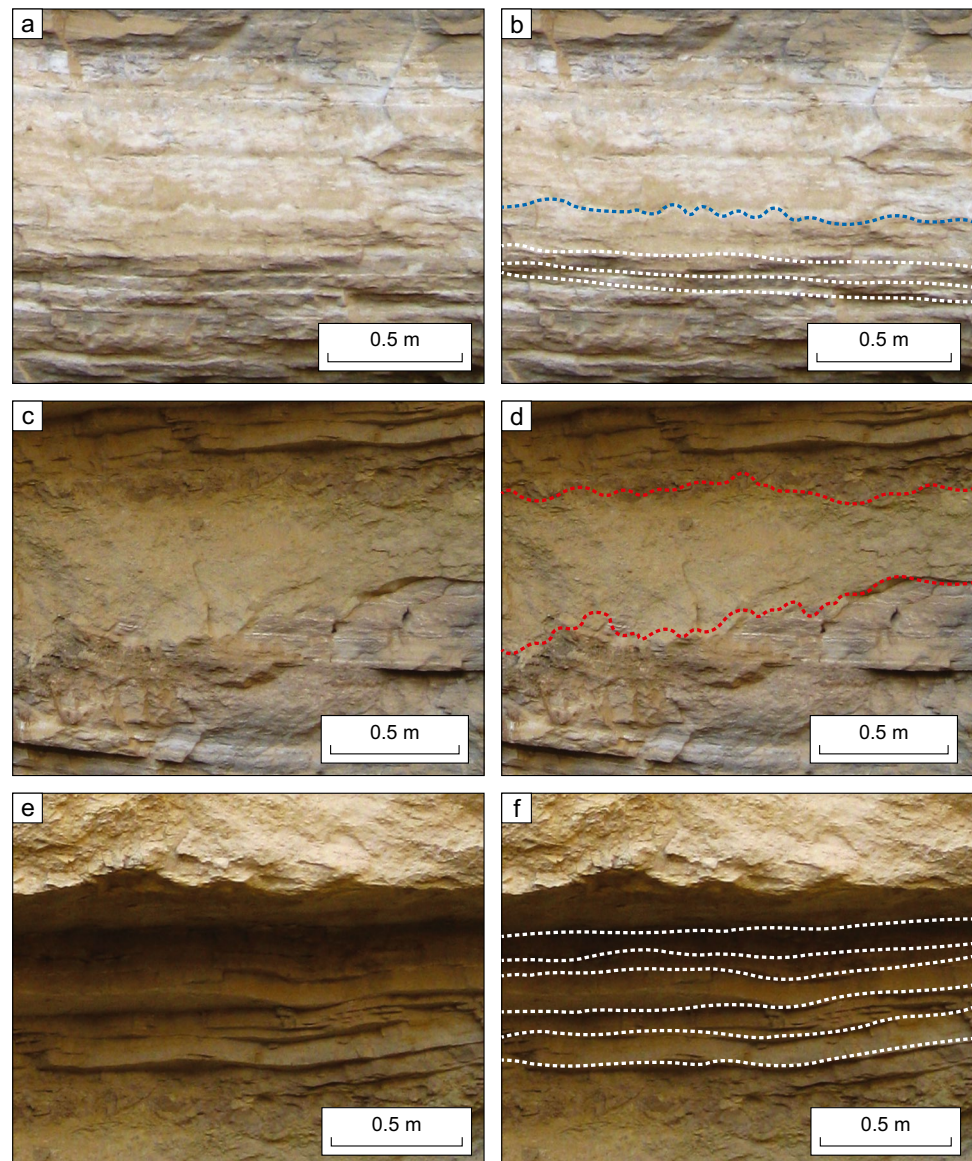
Fig. 8 Detailed photos and interpretations of the main sedimentological intervals in Fig. 6, continuing from Fig. 7 upwards to the Sulaiy Formation. **a** Breccia 2 bed is up to 2 m thick and **b** composed of very large, angular clasts up to several decimeters in size; the breccia is inversely sorted as marked in yellow. **c** The deformed anhydrite beds characterize the overlying interval, and **d** is highly deformed, as indicated by the black lines. **e**, **f** The evenly bedded limestones represent the lower Sulaiy Formation
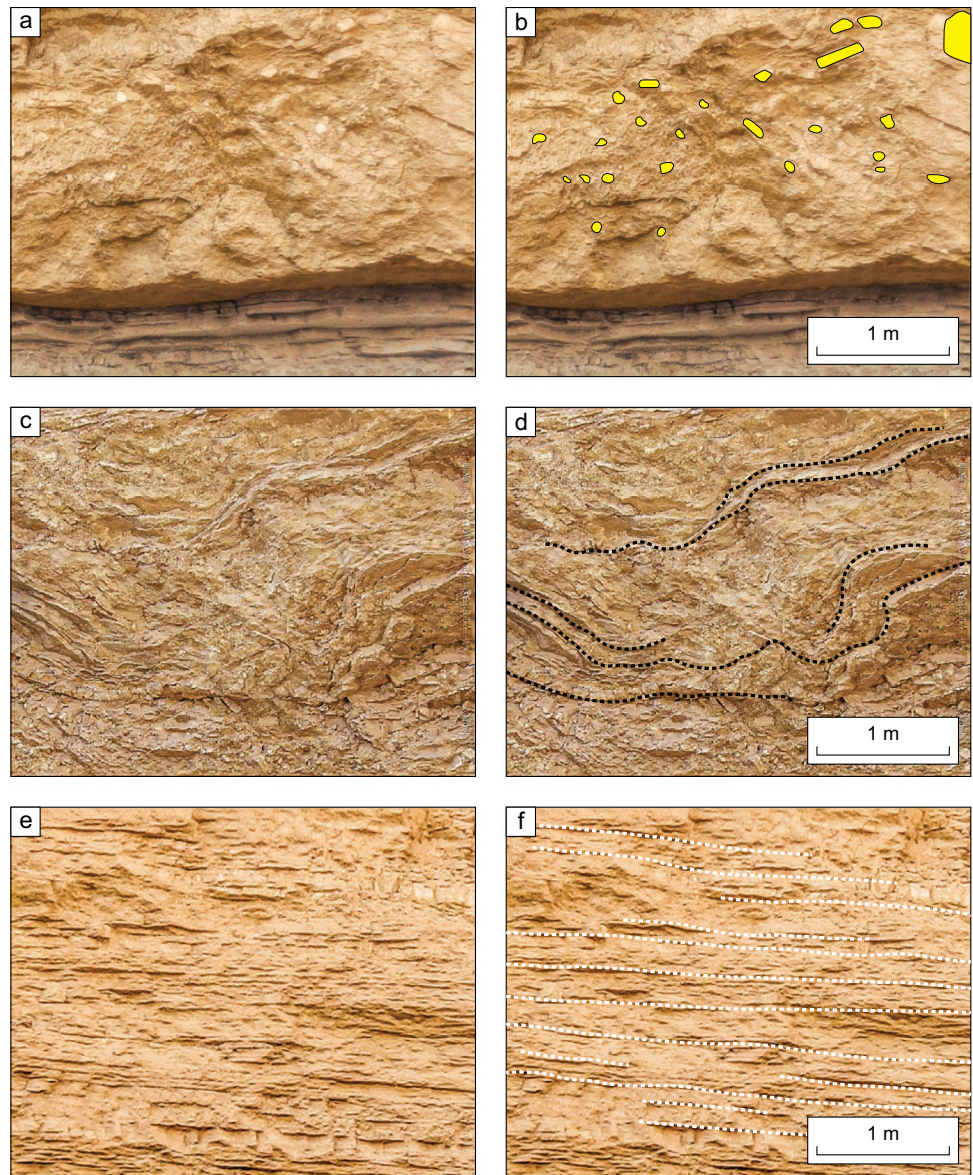

Fig. 9 Sedimentary structures and facies codes

Sedimentary structures	Facies Codes
Wave-ripples (Dolomite)	LFT 7: Dolomite
Massive (Anhydrite)	LFT 6: Massive Anhydrite
Laminated (Anhydrite)	LFT 5: Laminated Anhydrite
Chicken wire small (Anhydrite)	LFT 4: Tepee dominated Anhydrite
Chicken wire large (Anhydrite)	LFT 3: Microbial mats
Enterolithic (Anhydrite)	LFT 2: Nodular Anhydrite (separated)
Fine laminated (Microbial)	LFT 1: Nodular Anhydrite (touching)

Fig. 10 Facies types and main characteristics

Facies Code	Facies	Sedimentary structures	Thickness
LFT 1	Nodular Anhydrite (nodules touching)	chicken wire structures, nodules >3 cm	m to several m
LFT 2	Nodular Anhydrite (nodules separated)	chicken wire structures, nodules 1–3 cm	m to several m
LFT 3	Tepee dominated Anhydrite	Tepees, enterolithic structures	m to several m
LFT 4	Microbial mats	Very fine lamination	cm thick layers
LFT 5	Laminated Anhydrite	Lamination	m to several m
LFT 6	Massive Anhydrite	massive	dm to m
LFT 7	Dolomite Layer	Wave ripples, amalgamated sheets	dm to m

Fig. 11 Lithofacies type 1 (LFT 1): nodular anhydrite (nodules touching), commonly described as "chicken-wire" (pencil for scale in both photos). LFT 1 differs from LFT 2 in which the nodules are separated (Fig. 12)
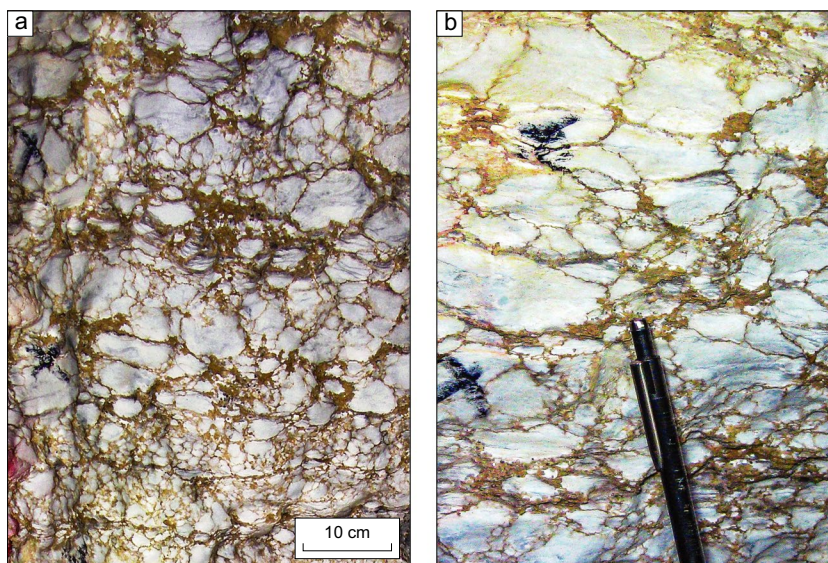
Interpretation Chicken-wire anhydrite can form in a sabkha or playa environment (Butler et al. 1982) caused by intrasedimentary growth, due to high evaporation rates and an upward movement of porewater. Alsharhan and Kendall (1994) compare these anhydrites to Holocene sediments described by Shearman (1966) and conclude they formed within the capillary zone in an arid, supratidal setting. The LFT 1 touching anhydrite nodules most likely formed under stable conditions during a longer period and could grow to larger nodules compared to LFT 2.

LFT 2: nodular anhydrite (nodules separated)

Observation Two types of nodular anhydrite with chicken-wire structure can be distinguished at the Dahal Hit outcrop. Unlike LFT 1 with its larger and touching anhydrite nodules, LFT 2 anhydrite nodules are smaller (c. > 3 cm) and separate (Fig. 12). The matrix between the anhydrite nodules was investigated and described by Leeder and Zeidan (1977) as quartz silt–rich, dolomitized grainstone hosts.

Interpretation A possible explanation for this observation could be the available time for the anhydrite nodules to grow within the capillary zone. The growth of the smaller and separated anhydrite nodules (LFT 2) was limited either by a shorter period of time and/or changing depositional conditions.

LFT 3: tepee-dominated anhydrite

Observation The laminated anhydrite often shows intervals dominated by tepee structures and enterolithic folds (Fig. 13).
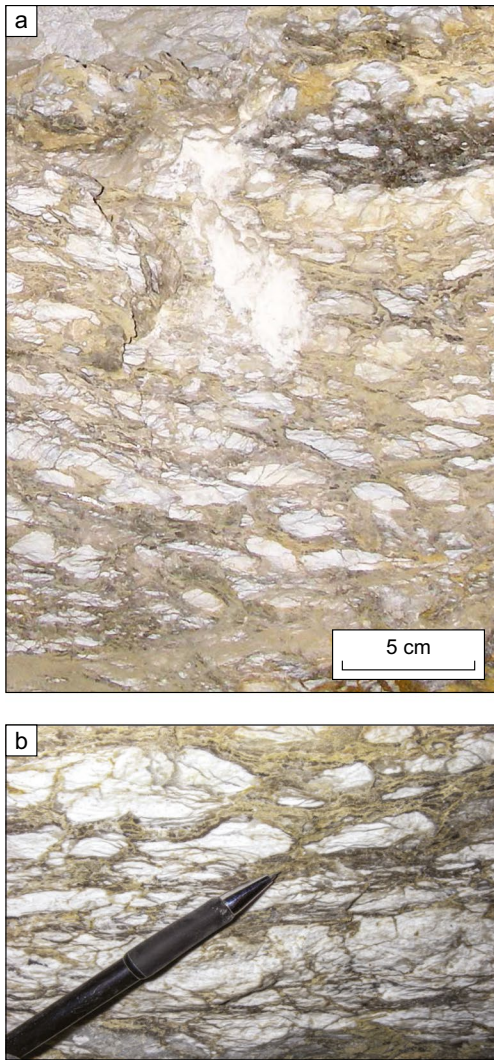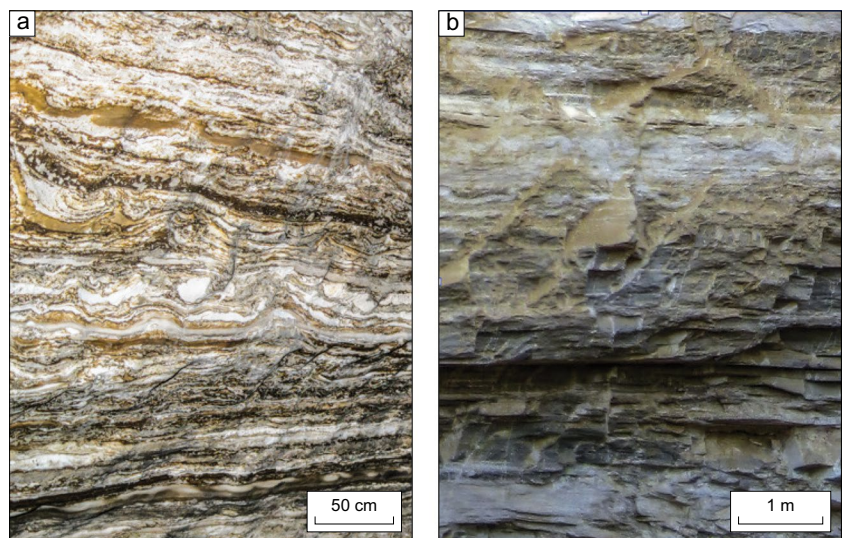
Fig. 12 Lithofacies type 2: nodular anhydrite (nodules separated)

Fig. 13 Lithofacies type 3: tepee-dominated anhydrite

Interpretation Tepee structures are indicators of exposure and range in vertical thickness from centimeters to decimeters. Enterolithic folds are a result of displacive intra-sedimentary growth (Alsharhan and Kendall 1994). Tepee-dominated anhydrite is associated with a very shallow subaqueous depositional environment, where laminated gypsum was precipitated. Occasional periods of exposure resulted in the formation of tepee structures. According to West (1979), if a flat gypsum sheet is present in sediment with minimal overburden (similar to modern sabkhas), it will expand through buckling in a direction perpendicular to the sheet after being hydrated.

LFT 4: microbial mats

Observation This facies type represents very fine laminated (millimeters) dolomitic layers, often only several centimeters in thickness (Fig. 14). LFT 4 was only observed in one interval of the investigated 28.5 m of outcrop section at Dahl Hit.

Interpretation Alsharhan and Kendall (1994, 2003) observed recent algal mats/peat on the coastal sabkha flats in Abu Dhabi and Macleod (Australia), as part of evaporite cycles. They are associated with an intertidal depositional environment and are part of the vertical relationships of the Holocene evaporites and carbonates.

LFT 5: laminated anhydrite

Observation This facies type formed depositional intervals with a thickness of several decimeters up to tens of meters and dominates the upper part of the Hith Formation at Dahl Hit (Fig. 15). The lamination itself is fine with a variation from several millimeters to centimeters. The fine lamination is very regular and shows a great lateral extent.

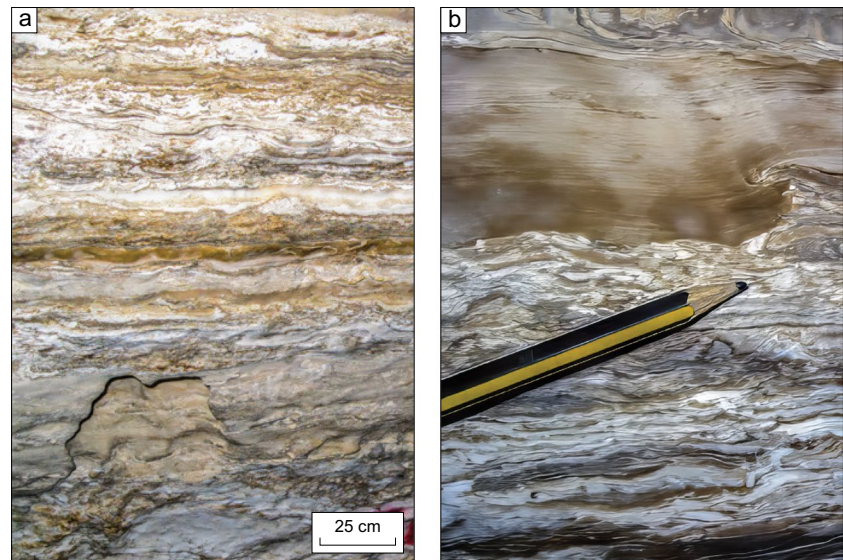**Fig. 14** Lithofacies type 4: very fine laminated microbial mats

Fig. 15 Lithofacies type 5 (LFT 5): laminated anhydrite. **a** View of the entrance to the Dahal Hit cavern showing the upper Hith Formation is dominated by LFT 5 intervals, which can be several 10 s of meters thick. **b** Well-exposed laminated anhydrite (previous gypsum) is related to the deposition within a very shallow, subaqueous environment
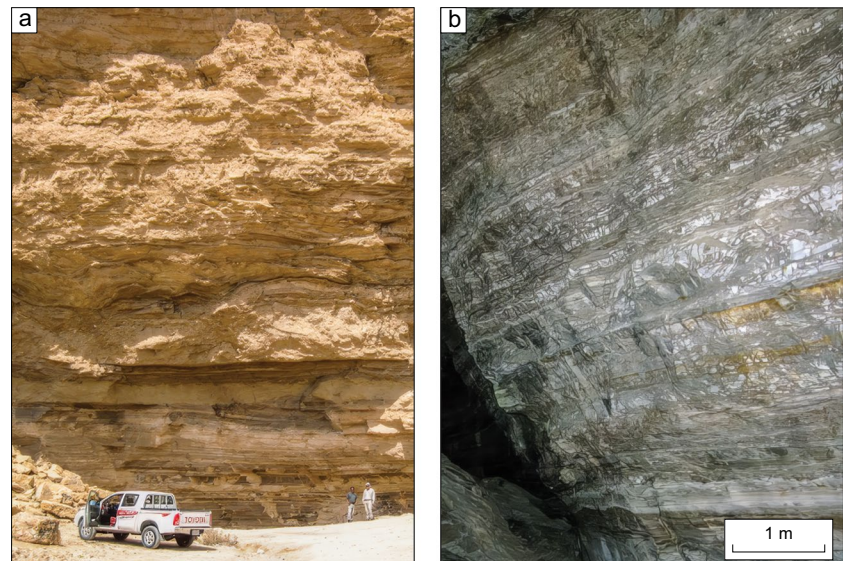
Interpretation The great lateral extent indicates a very flat relief. The laminated anhydrite is associated with deposition in a very shallow, subaqueous environment. Precipitation was primarily as laminated gypsum (e.g., laminated selenite, see Warren and Kendall 1985), and due to dehydration, the gypsum was converted into anhydrite.

LFT 6: massive anhydrite

Observation Massive anhydrite is decimeters to meters in thickness and shows almost no internal structure. Due to the lack of diagnostic features, it is difficult to assign it to a depositional environment.

Interpretation Alsharhan and Kendall (1994) suggested that deposition in a subaqueous salina or playa environment is most likely (Table 1). Warren and Kendall (1985) discussed the effect of diagenesis and the preservation potential of the primary sedimentological structures and textures in the geological record. They state that any subaqueous gypsum which is buried between 500 and 600 m will lose its original depositional texture as the gypsum dehydrates to nodular and massive anhydrite. Their fig. 5 shows, for example, the conceptual conversion of palmate ("siva") gypsum into nodular anhydrite.

In the Dahal Hit cavern, LFT 6 shows faint traces of bedding, which could be remnants of the original sedimentary structure (Fig. 16). Although speculative, the massive

Table 1 Criteria for subaerial versus subaqueous settings after Alsharhan and Kendall (1994), modified from Warren and Kendall (1985). Observations made in the present study are marked in bold

| Sabkha (subaerial)	Salina and playa (subaqueous)
Progradation	Aggradation
Along strike continuity	Concentric bands
Peritidal	**Isolated basin**
Low beach ridges	High coastal dunes
Flood recharge	Resurging groundwater
Carbonate-matrix dominated	**Evaporite dominated, minor carbonate matrix**
Nodular and enterolithic anhydrite	**Massive, laminated, or rippled gypsum**
Replacive and displacive evaporite	Bottom-nucleated evaporites
Algal mats (intertidal)	Stromatolites (subaqueous)
Localized tepees	**Extensive tepees**
Penecontemporaneous dolomite	Aragonite, calcite, and minor dolomite
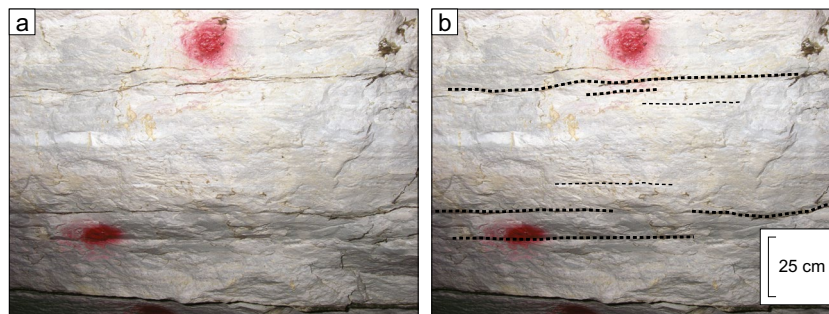
Fig. 16 Lithofacies type 6 (LFT 6). **a** The massive anhydrite shows some faint traces of bedding highlighted in photo **b**, which could be remnants of the original sedimentary structure. It remains specula-tive, but the massive anhydrite might have been a laminated gypsum/anhydrite deposited in a shallow subaqueous environment and was converted by diagenesis into massive anhydrite

anhydrite might have been a laminated gypsum/anhydrite deposited in a shallow subaqueous environment and was converted by diagenesis into massive anhydrite.

Transitional lithofacies

In the Dahal Hit cavern, we observed a potential "transitional" facies type that retains original facies types (e.g., lamination, bedding, teepee structures). The transitional facies type combines lamination (subaqueous) and nodular textures (subaerial) and hence cannot be associated with a depositional environment. This facies type might be a diagenetic overprint as discussed in Warren and Kendall (1985).

The photo in Fig. 17a shows an example of laminated anhydrite (LFT 5) and teepee structures (Fig. 17b). This transitional facies type has clearly preserved the primary sedimentary structures. It was initially deposited as laminated gypsum in a very shallow subaqueous environment and temporarily exposed as evident by the teepee structures.

The photo in Fig. 17c shows another example of the transitional facies type. The interval is layered but not finely laminated. Instead, the texture of the layers consists of white nodules, some of which are surrounded by thin rims. The texture approximately resembles the "chicken-wire" matrix associated with intra-sedimentary growth of gypsum/anhydrite nodules. If this transitional facies is a diagenetic overprint, the thin separation of these nodules could be impurities, as described by Warren and Kendall (1985) when gypsum crystals dehydrate into anhydrite.

However, it may be over-simplification to associate all the nodular anhydrite textures as a purely diagenetic product. Warren and Kendall (1985) state that the depositional cycle/sequence and vertical stacking of facies types need to be taken into account. In general, the investigated outcrop section at Dahl Hit shows a high cyclicity (see the "Cycles in Dahl Hit cavern" section), with sharp contacts, well-preserved sedimentary structures, and vertical stacking of facies types that are unlikely a purely diagenetic product.

LFT 7: dolomite layer

The photo in Fig. 18 shows an example of an intra-Hith dolomite layer interbedded between nodular anhydrite with a chicken-wire texture, reproduced from fig. 11 of Alsharhan and Kendall (1994). They interpret the formation of dolomite

Fig. 17 Examples of transitional facies types. **a**, **b** Laminated anhydrite (LFT 5) deposited as gypsum in a shallow marine setting with teepee structures indicating temporary exposure. **c**, **d** Massive anhydrite with layers showing nodular texture that resembles LFT 2 "chicken-wire" facies. The absence of fine lamination suggests gypsum crystals may have become dehydrated and converted to anhydrite
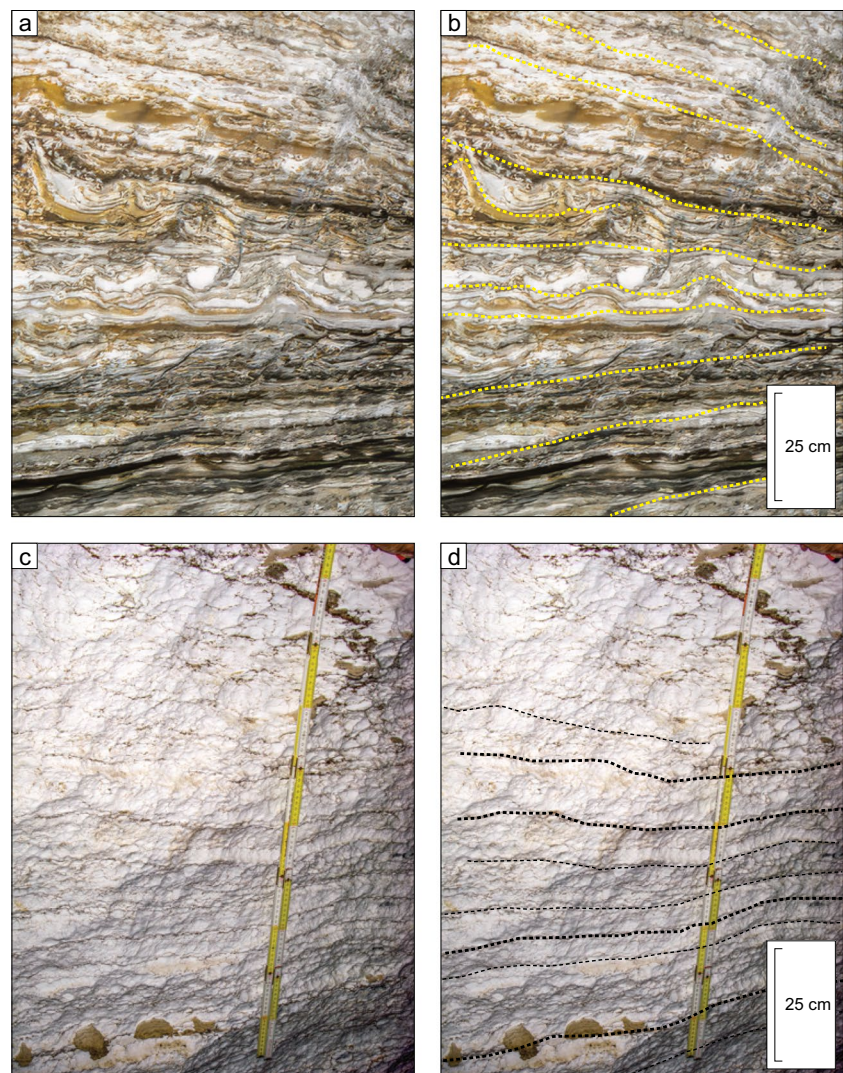
and nodular anhydrite as "pumping" of evaporites in a subaerial sabkha environment.

Observation In the present study, we made additional observations regarding intra-Hith dolomite layers (Fig. 19). The dolomite layers are laterally very continuous; however, they are internally composed of amalgamated sheets which continue for several 10 s of meters and are 10 to 30 cm thick. Well-preserved wave ripples are the dominant sedimentary structures.

Interpretation The wave ripples clearly indicate deposition in a subaqueous environment, and most likely represent flooding intervals. Additionally, the dolomite layers overlie the laminated anhydrite, which is already an indication of a very shallow subaqueous environment.

An important difference between supratidal and subaqueous dolomite could be the potential geometry of the geobodies. Whereas subaqueous dolomite layers seem to have sheet-like geometries, supratidal dolomites have facies-belt geometries. Because this study is based on outcrop observations at Dahl Hit, the interpretation is a general assumption and does not include regional well data for further evaluation.

Depositional model

The depositional environment of the Hith Formation has been the subject of several studies and discussions (Murris 1980; Alsharhan and Kendall 1994; Hughes et al. 2009; Wilson 2020). Before focusing on the depositional setting, it is important to understand the regional context and the development of the Arabian intra-shelf basin during the Jurassic. The evolution of the basin and the importance of the barrier towards the Neo-Tethys Ocean in the east is discussed in detail by Wilson (2020) and sketched in Fig. 20.

During the Jurassic, the intra-shelf basin tilted to the west resulting in increased accommodation space and thickness

Fig. 18 Dolomite layer associated with a sabkha environment from the Dahal Hit cavern documented by Alsharhan and Kendall (1994). The scale bar is 1 m. The dolomite layer is embedded into nodular anhydrite with a chicken-wire texture
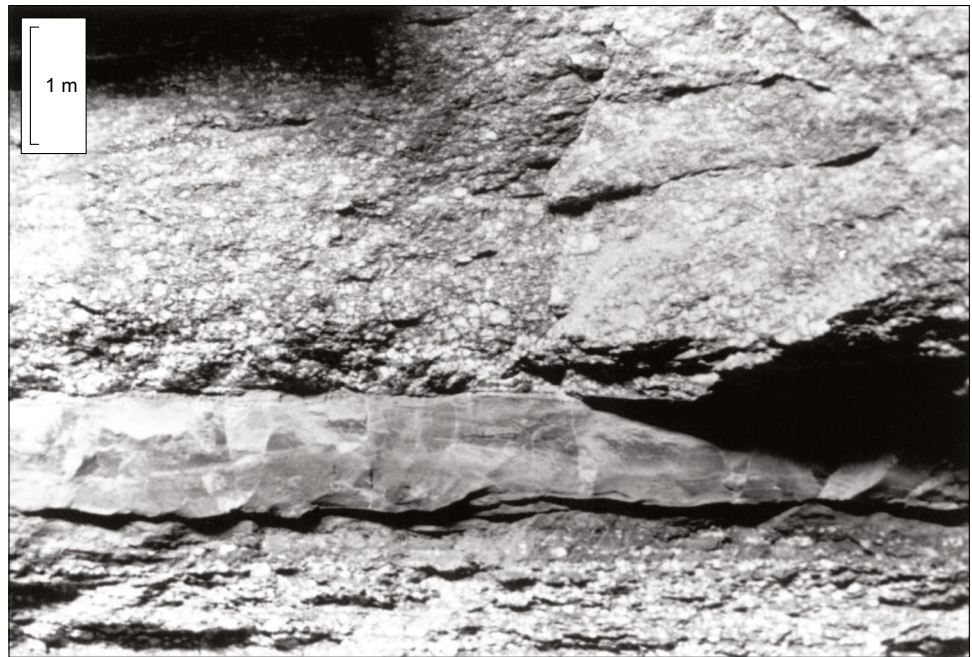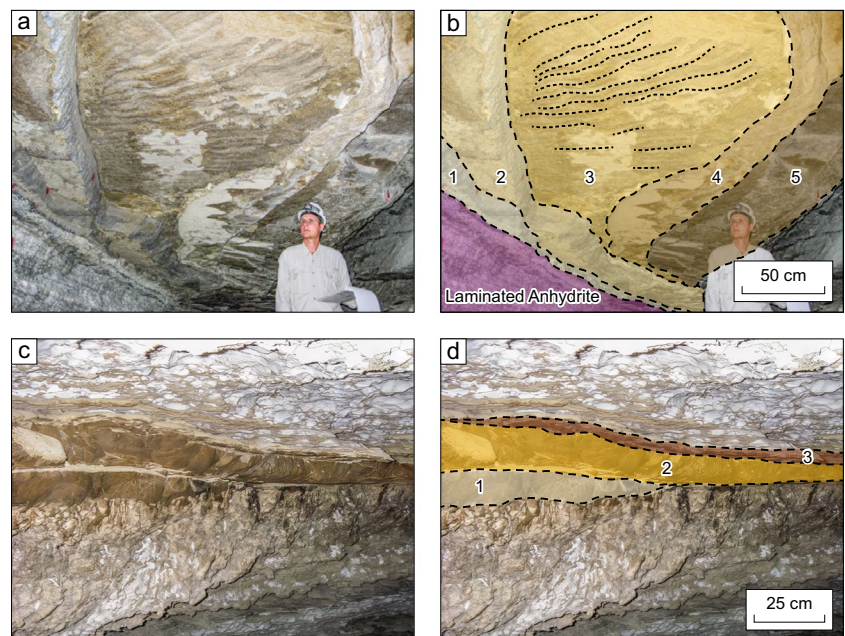

Fig. 19 **a** Dolomite layers at the top of the investigated section at 0.0–0.8 m in uppermost cycle 4 (Fig. 5). **b** Five amalgamated sheets (1–5) as well as well-developed wave ripples at the base of each sheet (black dashed line in amalgamated sheet 3). **c**, **d** Dolomite layers at 23.20 m in the middle of the lower cycle 1 (Fig. 5) composed of amalgamated sheets (1–3)


of the Hith Formation in the west towards the location of the Hith outcrop area (this study). A 200–300-km-wide shallow barrier in the east controlled the connectivity to the Neo-Tethys Ocean. When the barrier was effective, the basin was restricted leading to gypsum-anhydrite deposition, and when the barrier was flooded, carbonates precipitated and prograded to the west. Strong paleo-trade winds controlled the energy levels in the basin leading to a wind-driven water flow from east to west. Vahrenkamp et al. (2015) concluded that the widespread deposition of Arab and Hith anhydrites

are further evidence for tectonically driven basin isolation and evaporitic conditions in combination with eustatic sea-level fluctuations.

Azer and Peebles (1998) and Warren (2006) considered the depositional setting of the Hith Formation as a saltern with subaqueous evaporite beds extending across 100 s of kilometers. Warren and Kendall (1985) identified mixed sabkha and submarine and playa-like conditions in the Arabian Platform region for the Hith Formation. Alsharhan and Kendall (1994) suggested the nodular

Fig. 20 Depositional model showing the geometry and development of the intrashelf basin during the latest stage and the deposition of the Hith Formation (modified from Wilson 2020)

Sequence-stratigraphic interpretation

Review of interpretations
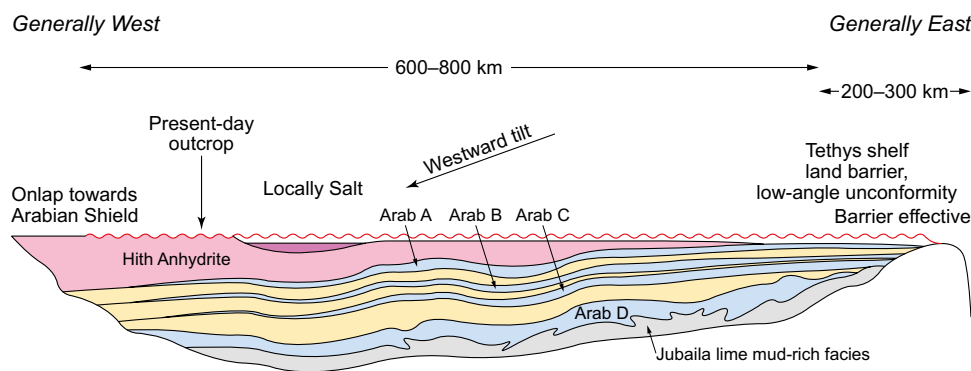
anhydrite formed within the capillary zone of an arid, supratidal setting whereas the laminated anhydrite probably accumulated in a subaqueous playa setting. They also proposed the existence of a north–south-oriented carbonate/sabkha barrier along the eastern and southern margins of the Arabian Platform, towards the Neo-Tethys Ocean. This proposed setting is supported by the presence of laminated anhydrite in much of the Hith Formation and the lack of abundant carbonates.

The extent of the Hith Anhydrite indicates that the marine setting was spread out farther than the underlying Oxfordian-Kimmeridgian Arab Formation (Wilson 2020). This extensive depositional setting is consistent with a steady rise in relative sea levels throughout the Late Jurassic. Despite the rise in sea level, Wilson (1985, 2020) recognized that the Upper Jurassic Arab carbonate-anhydrite cycles and overlying Hith anhydrite represent the most restricted phase of Jurassic sedimentation. They were the culmination of the progressive infilling of an open-marine shelf with a regressive sabkha and playa complex that was punctuated by brief, more open-marine episodes expressed as transgressive carbonate cycles. Table 2 shows a summary of facies types observed in this study and the relationship between the depositional setting and the status of the barrier towards the Neo-Tethys Ocean.

Several studies have interpreted the Hith Formation in terms of system tracts. Le Nindre et al. (1990) concluded that the Hith Formation has a subaqueous origin associated with restricted conditions during the late highstand. Al-Husseini (1997, his fig. 12) suggested that the Hith evaporites could have formed during both the late transgressive system tract and the early highstand, accumulating landwards of the Arab-A and Asab carbonates. Azer and Peebles (1995, Figs. 5 and 6; 1998) described five parasequences (fourth/fifth order?) for the Hith Formation in Abu Dhabi and interpreted them as transgressive hemicycles.

Hughes et al. (2009) discussed the paleoenvironment of the Hith Formation focusing also on sedimentological and micropaleontological evidence in the Manifa Field. They divided the Hith Formation into three members and considered it a second-order sequence named the "Manifa sequence." They interpreted the lower "anhydrite" member as the lowstand system tract and represent hypersaline subaqueous deposition within a restricted deep basin. Their middle "transitional" member is comprised of interbedded anhydrite and carbonates and corresponds to the transgressive system tract. Their upper "carbonate"

Table 2 Summary of results

Facies	Setting	Dimension	Figure	Barrier
LFT 1, LFT 2 nodular anhydrite	Sabkha (subaerial)	Several dm to 10 s of m thick	11 and 12	Closed
LFT 3 teepee-dominated anhydrite	Sabkha/salina, intermittent exposure (subaerial)	cm to dm thick	13	Intermittently open
LFT 4 microbial mats	Intertidal to peritidal (subaqueous)	Several cm thick	14	Open
LFT 5 laminated anhydrite	Extensive salina, very shallow (subaqueous)	Several dm to 10 s of m thick	15	Open
LFT 6 massive anhydrite	Indeterminate	Several dm to m thick	16	Indeterminate
LFT 7 dolomite	Flooding interval (subaqueous)	0.2–>1 m thick, 100 s m extent	18 and 19	Open

member consists of prograding shallow-marine units that represent the highstand system tract. The investigated section correlates most likely to the transitional or lower part of the carbonate member of the Hith Formation.

Hughes et al. (2009) further subdivided the Manifa sequence into third- and fourth-order sequences but remained undecided as to whether the anhydrite intervals represent the sea-level lowstands and transgressions, or the highstands and regressions. The lower third-order sequence represents the "anhydrite" and "transitional" members and the lowermost part of the "carbonate" member (option 1). This sequence is composed of three higher-frequency sequences (1A, 1B, and 1C). The upper third-order sequence is composed of four fourth-order sequences (labelled 2A, 2B, 2C, and 2D.

Alsharhan and Scott (2000) describe the Hith Formation as the final regressive, supratidal stage of the last major Jurassic cycle. Alsharhan and Whittle (1995) and Alsharhan and Kendall (1994) characterized the Dahl Hit type locality as follows: "The anhydrite has a chicken-wire texture with some dolomite in the lower part of the section, grading upward to a similar nodular texture and becoming laminated at the top including some fine-grained carbonate material." However, the overall increase of carbonate layers (from anhydrite to transitional and carbonate member) can also be interpreted as increasing transgressive events, where a permanent trend of sea-level rise leads to an end of the marine isolation and the dominance of evaporite deposits of the Arabian Intrashelf Basin (Wilson 2020; Hughes et al. 2009, Le Nindre et al. 1990).

Al-Husseini (2009) interpreted the Arab-A and main Hith interval as one depositional sequence separated by sequence boundaries SB 10 and SB 10.6 following the concept of the Arabian Orbital Stratigraphy (AROS), which calibrates the MFS and sequence boundaries (SB) based on the model of Al-Husseini and Matthews (2008). This leads to a duration of 2.8 Myr for the Arab-A and main Hith sequence (excluding the Manifa reservoir).

Cycles in Dahl Hit cavern

The following sequence-stratigraphic interpretation focuses on the logged 28.5 m outcrop section in the Dahl Hit cavern (Fig. 5). It shows three transgressive–regressive cycles and one transgressive hemicycle, with thicknesses of up to 10 m. The stratigraphic position of the logged section in relation to the top of the Arab Formation and to the Hith Formation in boreholes is not constrained. As such, it is not possible to integrate our interpretation with the second- and third-order sequence-stratigraphic frameworks of other authors (e.g., Hughes et al. 2009; Wilson 1985).

Cycle 1, Observation Cycle 1 is 9.8 m thick. An approximately 0.3-m-thick dolomite layer marks the base of this cycle. It is overlain by 3.5 m of nodular anhydrite with a chicken-wire texture and a 0.5-m-thick layer of massive anhydrite. The massive anhydrite quickly grades into an 80-cm-thick interval of laminated anhydrite, and a 0.3-m-thick wave ripple-dominated dolomite sheet marks the top of the succession and represents the turning point. From then onwards, the facies stacking shifts again and nodular anhydrite with a chicken-wire texture dominates the regressive succession, which is 4.8 m thick.

Interpretation The transgressive part of cycle 1 is interpreted as a shift from a sabkha environment represented by the nodular anhydrite to a subaqueous environment indicated by laminated anhydrite. The wave-ripple-dominated dolomite is also interpreted as subaqueous and represents an amalgamation of event deposits. The regressive part of cycle 1 is reflected by a fast transition to nodular anhydrite with a chicken-wire texture again, interpreted as sabkha deposits.

Cycle 2, Observation Cycle 2 is 6.7 m thick. The lower part is composed of 0.8 m of nodular anhydrite, followed by 0.9 m of laminated anhydrite with tepee structures and enterolithic folds. The succession is overlain by very thin (centimeter thick) fine-laminated microbial mats which alternate with laminated anhydrite (1.8 m). The maximum flooding interval is expressed as facies "turnaround" (Schlager 2005; Pawellek and Aigner 2004), rather than a distinct interval or surface. 3.2 m of laminated anhydrite follows the succession with an increasing presence of tepee structures towards the top.

Interpretation The base of cycle 2 is associated with the presence of nodular anhydrite and deposition in a sabkha environment. A shift of facies types to tepee-dominated anhydrite and fine-laminated microbial mats along with laminated anhydrite is interpreted as subaqueous deposits and therefore as a transgressive hemicycle. The maximum flooding surface is not a sharp layer or interval, but rather a turning point represented by laminated anhydrite and abundant tepee structures at the top of the succession. This is interpreted as a regressive hemicycle where the tepee-dominated interval represents exposure and the upper boundary of cycle 2.

Cycle 3, Observation Cycle 3 is 7.0 m thick. It is dominated by a 5.0-m-thick interval of laminated anhydrite, overlain by a 1.1-m-thick interval of massive anhydrite along with a 0.9-m-thick zone of nodular anhydrite with a chicken-wire texture.

Interpretation The relative thick interval of laminated anhydrite is interpreted as a transgressive hemic cycle. No tepee structures or enterolithic folds were observed. This indicates stable subaqueous depositional conditions for a longer period. The transgressive hemicycle clearly dominates the character of cycle 3. The regressive hemic cycle is represented by massive anhydrite and nodular anhydrite with chicken-wire textures associated with a sabkha environment.

Cycle 4, Observation Cycle 4 is 4.5 m thick. It starts with nodular anhydrite at the base and grades into massive anhydrite (1.0 m) followed by laminated anhydrite (3.0 m). An over 1.0-m-thick dolomite layer with wave-ripple structures represents the top of the logged interval.

Interpretation Cycle 4 is interpreted as a transgressive hemicycle, which evolves from nodular anhydrite at the base (sabkha) to laminated anhydrite to dolomite with wave ripples (transgressive events) at the top. The 3.0-m-thick laminated anhydrite interval is interpreted as subaqueous deposits, and the maximum flooding interval is represented by the dolomites.

This interpretation implies that dolomitization is not only associated with a supratidal environment in the Hith Formation (Alsharhan and Kendall 1994) but is also well developed in transgressive deposits. A possible important difference between supratidal and subaqueous dolomites could be the geometry of these geobodies. Whereas subaqueous dolomite layers have sheet-like geometries, supratidal dolomites have facies-belt geometries.

Fractures and internal deformation

Three types of internal deformation features were observed in the Hith Formation (Fig. 21): (1) decimeter thick brecciated shear zones, (2) slickensides, and (3) small-scale faults/folds (centimeter to decimeter thick) were commonly observed at major facies boundaries. These features tend to develop at the contact between nodular and the laminated anhydrites, which may represent a major change in geomechanical properties. The orientation is typically bedding-parallel to sub-parallel.

No open or partially open fractures were observed in the outcrop section. Also, the brecciated layer interpreted as a fault/fracture damage zone shown in Fig. 21a has no visible porosity and permeability due to the tight character of the anhydrite-dominated matrix and the horizontal orientation of the feature. Figure 21b shows a slickenside, which was frequently observed within the laminated anhydrite intervals. It shows that some sections of the Hith Formation are relatively unstable (e.g., the laminated anhydrite) and react with bedding-parallel shear movements to stress. Other
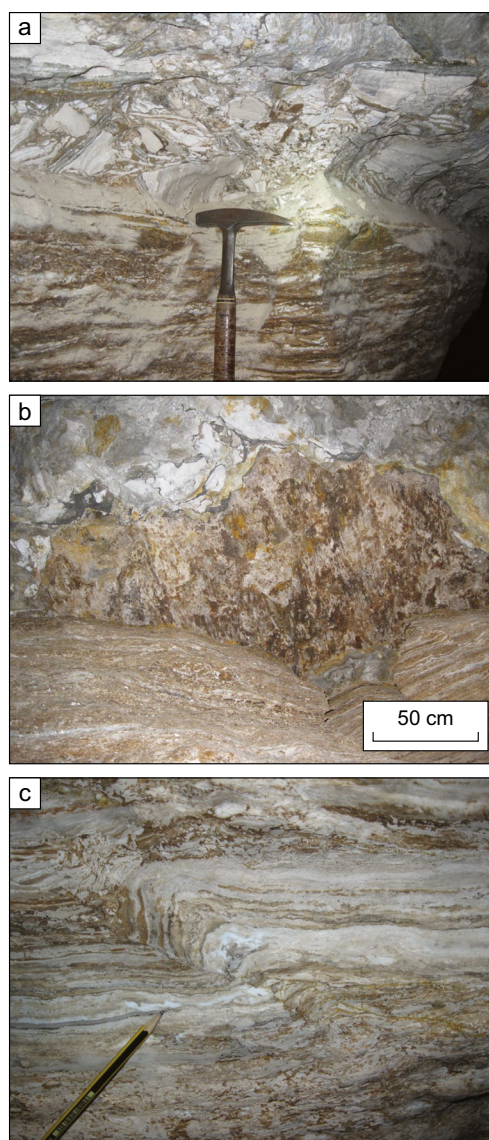
Fig. 21 Examples of deformation features in the Hith Formation: **a** brecciated shear zone, **b** slickenside within the laminated anhydrite interval, and **c** small-scale fault and fold

intervals, especially the nodular anhydrite, are more "massive" in texture and show almost no fractures or internal deformation features (Fig. 21c).

Summary and conclusions

A 28.5-m interval in the exposed section of the Tithonian Hith Anhydrite Formation in the Dahal Hit cavern in Saudi Arabia was investigated. The interval represents approximately one-third of the 90-m-thick formation, but its stratigraphic position above the top of the Arab Formation is not constrained. Seven facies types were identified in the

interval, and their depositional environments are interpreted as alternating between salina (subaqueous) and sabkha (subaerial). The vertical stacking patterns of the facies reveal three complete transgressive–regressive cycles with thicknesses of up to 10 m, and the lower part of a fourth cycle that likely extends above the logged section. The facies analyses show faint traces of laminations in the massive anhydrite, which suggests it was deposited in a subaqueous environment and diagenetically altered.

Structural features, such as shear fracture and parallel-bedded deformation zones, were observed. They seem to have a very tight character and might not contribute to potential intra-Hith flow zones. However, more vertical fractures/faults could well provide fluid pathways, as known from the Manifa field, where hydrocarbons from the Arab Formation breached the seal and leaked into the Hith seal/reservoir. Similar observations were made in Qatar (Van Buchem et al. 2014).

The 50-m rise of the groundwater level in 6 years in the Dahal Hit cavern implied a well-connected karst and/or permeability network is present in the greater Ar Riyadh area, which most likely connects the cavern to the treated sewage water lakes situated 10 km to the south. The pathway of the water flow is most likely associated with anhydrite dissolution features along with possible karstification, as well as high-permeability flow zones present in dolomite layers. Dissolution features and high-permeability networks are also reported in subsurface studies of the Hith Formation. These observations highlight the importance of further studies related to the potential storage of CO_2 or other geo-energy applications, as there is clear evidence for fluid flow and pathways within the world's most prolific hydrocarbon seal, the Hith Anhydrite Formation.

Declarations

Competing interests The authors declare no competing interests.

References

Afifi AM (2005) Ghawar, the anatomy of the world's largest oil field. AAPG Search and Discovery Article No. 20026. https://www.searchanddiscovery.com/pdfz/documents/2004/afifi01/images/afifi01.pdf.html

Al-Husseini MI (1997) Jurassic sequence stratigraphy of the western and southern Arabian Gulf. GeoArabia 2(4):361–382

Al-Husseini M (2009) Update to late triassic-jurassic stratigraphy of Saudi Arabia for the middle east geologic time scale. Stratigraphic Note. GeoArabia 14(2):145–186

Al-Husseini MI, Matthews RK (2008) Jurassic-Cretaceous Arabian orbital stratigraphy: the AROS-JK chart. GeoArabia 13(1):89–94

Alsharhan AS, Kendall CGStC (1986) Precambrian to Jurassic rocks of Arabian Gulf and adjacent areas: their facies, depositional setting, and hydrocarbon habitat. Bulletin 70:977–1002

Alsharhan AS, Kendall CGStC (1994) Depositional setting of the Upper Jurassic Hith anhydrite of the Arabian Gulf: an analog to Holocene evaporites of the United Arab Emirates and Lake MacLeod of Western Australia. Bulletin 78:1075–1096

Alsharhan AS, Kendall CGStC (2003) Holocene coastal carbonates and evaporites of the southern Arabian Gulf and their ancient analogues. Earth Sci Rev 61:191–243

Alsharhan AS, Nairn AEM (1986) A review of the Cretaceous formations in the Arabian Peninsula and Gulf: Part I. Lower Cretaceous (Thamama Group) stratigraphy and paleogeography. J Pet Geol 9:365–391

Alsharhan AS, Scott RW (2000) Hydrocarbon potential of Mesozoic carbonate platform-basin systems, U.A.E. SEPM Spec Publ 69:335–358

Alsharhan AS, Whittle GL (1995) Carbonate-evaporite sequences of the Late Jurassic, southern and southwestern Arabian Gulf. Bulletin 79:1608–1630

Ayres G, Bilal M, Jones RW, Slentz RW, Tartir M, Wilson AO (1982) Hydrocarbon habitat in main producing areas, Saudi Arabia. AAPG Bull 66:1–9

Azer SR, Peebles RG (1995) Sequence stratigraphy of the Hith/Upper Arab formations offshore Abu Dhabi, U.A.E., SPE 29799

Azer SR, Peebles RG (1998) Sequence stratigraphy of the Arab A to C and Hith Formation offshore Abu Dhabi, UAE. GeoArabia 3:251–268

Butler GP, Harris PM, Kendall CGSt C (1982) Recent evaporites from Abu Dhabi coastal flats. In. C.R. Handford, G.L. Robert, & R.D. Graham (eds), Depositional and diagenetic spectra of evaporites (core workshop no. 3.):3364. Tulsa, Oklahoma, SEPM

Cohen KM, Finney SC, Gibbard PL snf Fan JX (2013; updated) The ICS international chronostratigraphic chart. Episodes 36: 199–204. http://www.stratigraphy.org/ICSchart/ChronostratChart2023-04.pdf

Farooq AS, Khan MS, Magara K (1991) Outcrop-subcrop sequence and diagenesis of Upper Jurassic Arab-Hith Formations , Central Saudi Arabia. JKAU: Earth Sci 4:105–136

Fedorik J, Delaunay A, Losi G, Panara Y, Menegoni N, Afifi AM, Arkadakskiy S, Al Malallah M, Oelkers E, Gislason SR, Ahmed Z, and Kunnummal N (2023) Structure and fracture characterization of the Jizan group: implications for subsurface CO2 basalt mineralization. Front Earth Sci Sec Struct Geol Tectonics 10 - 2022

Hughes GW, Al-Khalid M, Varol O (2009) Oxfordian biofacies and paleoenvironments of Saudi Arabia. Volumina Jurassica VI:47–60

Hughes GW, Naji N (2008) Sedimentological and micropalaeontological evidence to elucidate post-evaporitic carbonate palaeoenvironments of the Saudi Arabian latest Jurassic. Vol Jurass 6:61–73

Le Nindre YM, Manivit J, Vaslet D (1990) Stratigraphie séquentielle du Jurassique et du Crétacé en Arabie Saoudite. Bull Soc Géol Fr Paris 8(VI):1025–1034

Leeder MR, Zeidan R (1977) Giant Late Jurassic sabkhas of Arabian Tethys. Nature 268:42–44

Michelsen N, Dirks H, Schulz S, Kempe S, Al-Saud M, Schüth M (2016) YouTube as a crowd-generated water level archive. Sci Total Environ 568:189–195

Murris RJ (1980) Middle East: stratigraphic evolution and oil habitat. AAPG Bull 64:597–618

Oelkers EH, Arkadakskiy S, Afifi AM, Hoteit H, Richards M, Fedorik J, Delaunay A, Torres JE, Ahmed ZT, Kunnummal N, Gislason SR (2022) The subsurface carbonation potential of basaltic rocks from the Jizan region of Southwest Saudi Arabia. Int J Greenhouse Gas Control 120:103772

Pawellek T, Aigner T (2004) Dynamic stratigraphy as a tool in economic mineral exploration: ultra-pure limestones (Upper Jurassic, SW Germany). Mar Pet Geol 21(4):499–516

Powers RW (1968) Saudi Arabia. Lexique Stratigraphique International, V. III. Centre National de la Recherche Scientifique, Paris

Powers RW, Ramirez LF, Redmon CD, Elberg EI Jr (1966) Geology of the Arabian Peninsula: Sedimentary geology of Saudi Arabia. Professional Papers, 560D. https://pubs.usgs.gov/publication/pp560D; https://doi.org/10.3133/pp560D

Rausch R, Dirks H (2024) A hydrogeological overview of the Upper Mega Aquifer System on the Arabian Platform. Hydrogeol J. https://doi.org/10.1007/s10040-023-02760-0

Rausch R, Dirks H, Al Ajmi H (2013) Zur Hydrogeologie des „Oberen Mega-Aquifer-Systems" auf der Arabischen Halbinsel. – Jh. Ges. Naturkde. Württemberg, Sonderband, S. 119-145, 22 Abb., 2 Tab.; Stuttgart. https://www.researchgate.net/profile/Randolf-Rausch/publication/348153366_Auf_der_Suche_nach_dem_Wasser_der_Wuste/links/5ff09eb745851553a014e42f/Auf-der-Suche-nach-dem-Wasser-der-Wueste.pdf

Schlager W (2005) Carbonate sedimentology and sequence stratigraphy. Vol. 8, SEPM Concepts in Sedimentology and Paleontology. p 200. https://doi.org/10.2110/csp.05.08

Sharland PR, Archer R, Casey DM, Davies RB, Hall SH, Heward AP, Horbury AD, Simmons MD (2001) Arabian Plate Sequence Stratigraphy. GeoArabia Special Publication 2. Gulf PetroLink, Bahrain, p 371. https://www.researchgate.net/publication/279778628_Arabian_Plate_Sequence_Stratigraphy_GeoArabia

Shearman DJ (1966) Origin of marine evaporites by diagenesis. Trans Inst Mineral Metall Section B 75:208–215

Steineke M, Bramkamp RA, Sander NJ (1958) Stratigraphic relations of Arabian Jurassic habitat of oil. Am Asso Petrol Geol Bull 37:1252–1278

Vahrenkamp V, van Laer P, Franco B, Celentano MA, Grélaud C (2015) Late Jurassic to Cretaceous source rock prone intrashelf basins of the eastern Arabian Plate – Interplay between tectonism, global anoxic events, and carbonate platform dynamics. Extended abstract presented at the International Petroleum Technology Conference. Doha, Qatar. https://doi.org/10.2523/IPTC-18470-MS

Vahrenkamp V, Afif A, Tasianas A, Hoteit H (2021) The geological potential of the Arabian plate for CCS and CCUS - An overview. Proceedings of the 15th Greenhouse Gas Control Technologies Conference 15-18 March 2021. Available at SSRN: https://ssrn.com/abstract=3822139 or https://doi.org/10.2139/ssrn.3822139

Van Buchem FSP, Svendsen N, Hoch E, Pedersen-Tatalovic R, Habib K (2014) Depositional history and petroleum habitat of Qatar, in L. Marlow, C. Kendall and L. Yose, eds., Petroleum systems of the Tethyan region: AAPG Memoir 106:641– 677

Vaslet D, Al-Muallem MS, Maddah SS, Brosse JM, Fourniguet J, Breton JP, Le Nindre YM (1991) Explanatory notes to the geologic map of the Ar Riyad Quadrangle, Kingdom of Saudi Arabia. Geoscience map GM-121, scale 1:250,000, sheet 24I. Deputy Ministry for Mineral Resources, Ministry of Petroleum and Mineral Resources, Kingdom of Saudi Arabia, p 54. https://search.worldcat.org/de/title/geologic-map-of-the-ar-riyad-quadrangle-sheet-24-i-kingdom-of-saudiarabia/oclc/53923617

Warren JK (2006) Evaporites: sediments, resources and hydrocarbons. Springer, Berlin, p 1035p

Warren JK, Kendall CGStC (1985) Comparison of marine (subaerial) and salina (subaqueous) evaporites: modern and ancient. Am Assoc Petrol Geol Bull 69:1013–1023

West I (1979) Primary gypsum nodules in a modern sabkha on the Mediterranean coast of Egypt. Geology 7:354–358

Wilson AO (1985) Depositional and diagenetic facies in the Jurassic Arab-C and -D reservoirs, Qatif Field, Saudi Arabia. In: Roehl PO, Choquette PW (eds) Carbonate petroleum reservoirs. Springer-Verlag, New York, pp 319–340

Wilson AO (2020) The Middle to Late Jurassic Arabian Intrashelf Basin of the Eastern Arabian Peninsula. Geol Soc Memoir No 53:213p

Wolpert PJ, Bartenbach M, Suess MP, Rausch R, Aigner T, Le Nindre YM (2015) Facies analysis and sequence stratigraphy of the uppermost Jurassic-Lower Cretaceous Sulaiy Formation in outcrops of central Saudi Arabia. GeoArabia 20:67–122

Ziegler MA (2001) Late Permian to Holocene paleofacies evolution of the Arabian Plate and its hydrocarbon occurrences. GeoArabia 6(3):445–504